Aerosol Science and Technology, 38(S1):104–117, 2004

ISSN: 0278-6826 print / 1521-7388 online
DOI: 10.1080/02786820390229534

Measurement of Ambient Aerosol Composition During the PMTACS-NY 2001 Using an Aerosol Mass Spectrometer. Part II: Chemically Speciated Mass Distributions

Frank Drewnick,[1] John T. Jayne,[2] Manjula Canagaratna,[2] Douglas R. Worsnop,[2] and Kenneth L. Demerjian[1]

[1]*Atmospheric Sciences Research Center, State University of New York, Albany, New York*
[2]*Center for Aerosol and Cloud Chemistry, Aerodyne Research Inc., Billerica, Massachusetts*

Ambient particulate mass distributions (10 min averages) for nitrate, sulfate, ammonium, and organic particles were obtained during the deployment of the aerosol mass spectrometer (AMS) in the PM2.5 Technology Assessment and Characterization Study–New York (PMTACS–NY) in Queens, New York in summer 2001. Nitrate and sulfate particles were found to be internally mixed and mainly represented by ammonium nitrate and ammonium sulfate. Their average mass distributions are monomodal, with mode diameters of 440 nm and 450 nm and distribution widths around 600 nm. The maximum of the ammonium mass distribution was found at 400 nm and its width was about 550 nm. The average mass distribution of organic particles was bimodal with maxima at 80 nm and 360 nm and widths of 80 nm and 700 nm. While most of these distributions did not exhibit any significant diurnal patterns, the relative intensity of the small particle mode of the organic particles ($D_p <$ 120 nm) was found to be most intense during rush-hour times, indicating that the small organic particle fraction is mostly traffic related. Short-time averages of the size distributions, measured for different species independently, showed the ability of the AMS to track the growth and evolution of chemically distinct particles.

Received 23 October 2002; accepted 5 March 2003.

This work was supported in part by the New York State Energy Research and Development Authority (NYSERDA), contract # 4918ERT-ERES99; the US Environmental Protection Agency (EPA), cooperative agreement # R828060010; and New York State Department of Environmental Conservation (NYS DEC), contract # C004210. Although the research described in this article has been funded in part by the US Environmental Protection Agency, it has not been subjected to the Agency's required peer and policy review and therefore does not necessary reflect the views of the Agency, and no official endorsement should be inferred. We would like to thank Queens College for cooperation and logistical support during the campaign and NYS DEC for providing filter speciation data.

Frank Drewnick's current address: Institute of Atmospheric Physics, University of Mainz, D-55128 Mainz, Germany.

Address correspondence to Kenneth L. Demerjian, Atmospheric Sciences Research Center, SUNY Albany, 251 Fuller Road, Albany, NY 12203, USA. E-mail: kld@asrc.cestm.albany.edu

INTRODUCTION

In recent years atmospheric aerosols have received an increasing amount of attention due to their important role in physical and chemical processes in the atmosphere-like climate, forcing heterogeneous chemistry and cloud formation (Ravishankara 1997; Jacob 2000; Hizenberger et al. 1999) as well as their possible impact on human health (Finlayson-Pitts and Pitts 1997; Pope et al. 2002; Samet et al. 2000). Years of intensive research and development in the field of aerosol analysis has resulted in significant improvements in aerosol instrumentation. Nevertheless, there is a broad consensus in the community that the available data on ambient aerosol mass and chemical composition as a function of size are not adequate (McMurry 2000), especially for the organic aerosol fraction.

Off-line methods that traditionally have been used for characterization of atmospheric aerosols are based on sample collection techniques on filters and impactors, and subsequent analysis using multiple analytical techniques. These methods tend to suffer from sampling artifacts (Seinfeld and Pandis 1998; McMurry 2000) as well as low time resolution and high postcollection analysis costs.

A significant improvement of chemical analysis of atmospheric aerosols was accomplished by the development of laser vaporization/ionization aerosol mass spectrometers (Gard et al. 1997; Liu et al. 1995a, b; Murphy and Thomson 1997; Carson et al. 1997a) that provide information on the chemical composition of single particles. However, these techniques suffer from drawbacks inherent in their single-step vaporization/ionization process which lead to biases in particle-size representation and in the relative response to individual chemical species (Reilly et al. 1999; Gross et al. 2000; Allen et al. 2000; Kane and Johnston 2000), making them less than ideal for quantitative analyses. In addition, the detection in most of these instruments is limited to particles larger than about 0.2 μm due to the optical particle detection techniques required for laser triggering. However, a

few of the laser vaporization instruments analyze particles of smaller sizes by free firing of the laser without optical particle detection (e.g., Carson et al. 1997b).

In recent years a range of new ambient aerosol analysis techniques capable of providing quantitative on-line and almost real-time information on the chemical properties of particles has been developed, including on-line ion chromatographic techniques (Weber et al. 2001), or thermal evaporation techniques with subsequent gas analysis for sulfate, nitrate, and carbon mass concentration measurements (Stolzenburg and Hering 2000; Allen et al. 2000).

Another recently developed instrument is the aerosol mass spectrometer (AMS), developed and manufactured by Aerodyne Research, Inc. (Jayne et al. 2000; Jimenez et al. 2003). The AMS is capable of quantitative analysis of the nonrefractive aerosol components as well as measurement of species-resolved particle size distributions in near real-time, using thermal evaporation of the particles and subsequent electron-impact ionization and quadrupole mass spectrometry of the vapor.

The PM2.5 Technology Assessment and Characterization Study–New York (PMTACS–NY) 2001 is one of several US EPA "Supersites" intended to provide enhanced measurement data on chemical and physical composition of fine particulate matter and its precursors. One of the primary objectives of this study is to test and evaluate new measurement techniques for particulate matter. In pursuit of this goal, a wide variety of state-of-the-art on- and off-line techniques for physical and chemical aerosol analysis, including an AMS, have been deployed in a common field intensive at Queens College in New York City during July 2001.

In this article we describe the operation of the AMS during this campaign as well as data-processing procedures. Results of the mass weighed size distribution measurements obtained with this instrument are discussed. A discussion of mass concentration measurements with the AMS during PMTACS–NY 2001 is provided in companion article appearing this issue (Drewnick et al. 2003).

INSTRUMENT DESCRIPTION

Since we provided a more detailed description of the AMS in the first part of this article (Drewnick et al. 2003), we present here only a very brief overview of the instrument, focusing on the size-distribution measurement. A comprehensive description of the apparatus and its operation is given in Jayne et al. (2000).

The instrument consists of three differentially pumped vacuum chambers for particle sampling, particle sizing, and analysis. The ambient aerosol is introduced into the instrument through an aerodynamic particle beam-forming lens similar to that described by Liu et al. (1995a, b). Particles in the range of ~60 nm to 600 nm are focused and reach the detector with almost 100% efficiency, allowing a quantitative analysis of most of the accumulation-mode aerosol. In the vacuum the particle beam passes through a skimmer, a chopper, the particle sizing chamber of 30 cm length, and an aperture before it impacts on the heater surface, a mesh-coated molybdenum cartridge heater at about 700°C. After flash vaporization of the volatile and semivolatile particle components, the vapor is ionized by electron impact ($E_{el} = 70$ eV) and analyzed via a quadrupole mass spectrometer. The AMS is operated in two different modes: the "mass spec" (MS) mode of operation for quantitative analysis of the bulk composition of the nonrefractory aerosol components with no size information, and the "time-of-flight" (ToF) mode for species- and size-resolved mass distribution measurement at a limited number of masses. These modes of operation are explained in Part I, so here we will just repeat and focus on some details of the ToF mode used in the measurements presented in this report.

In the last orifice of the lens the sample flow undergoes a supersonic expansion, accelerating all particles in the air sample. Larger particles gain less velocity in this expansion than smaller particles because of their greater inertia, making aerodynamic sizing of the particles possible by measuring the particle time-of-flight, or velocity.

For particle sizing the chopper wheel (2% duty cycle, located right after the skimmer at the beginning of the sizing chamber) is moved into the particle beam, using a computer-controlled servo motor. The quadrupole mass spectrometer is set to a single mass, and the time-resolved ion signal during each chopper cycle is measured. The chopper position and detector are synchronized with a photodiode monitoring the chopper rotation. Since the evaporation, ionization, and analysis processes are fast (tens of μs) compared to the travel time of the particles through the chamber (some ms), the particle velocity distribution can be mapped out in this ToF mode. The particle velocity distribution is converted into a size distribution based on a calibration with polystyrene latex (PSL) and ammonium nitrate particles of known diameter. To measure the size distribution at a number of masses, the mass spectrometer setting is switched between selected mass settings after several chopper cycles.

Using this approach of measuring the time-resolved ion signal intensity of the particle vapor at selected masses after acceleration of these particles according to their aerodynamic properties, a direct measurement of mass distribution versus the aerodynamic diameter for the species associated with the masses selected for ToF analysis is obtained. All discussion of size distributions in this article refer to mass weighted distributions.

FIELD OPERATION AND DATA PROCESSING

During the PMTACS–NY 2001 summer intensive the AMS was operated at the measurement site at Queens College in Queens, New York from 30 June until 5 August. The measurement site was located at the edge of parking field #6 adjacent to an athletic field. Queens College (40.74° N, 73.82° W; altitude, ~25 m a.S.L.), located in the heart of Queens, is approximately a 100 m south of the Long Island Expressway and 1 km east of Van Wyck Expressway, two high-traffic highways in the New York City metropolitan area.

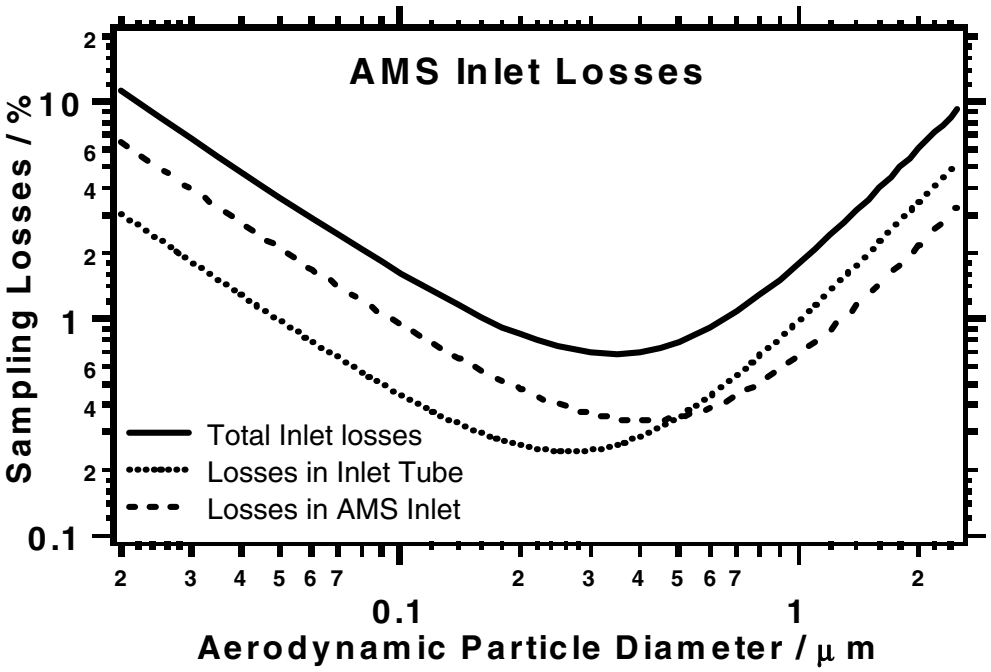

Figure 1. Inlet losses calculated for the inlet used in PMTACS–NY 2001 for the copper inlet tube to the instrument and for the AMS inlet itself, as well as the total losses, which also includes the losses in the isokinetic sampling probe.

The AMS was housed in an air-conditioned trailer together with other aerosol instruments. The sampling inlet was mounted on a tower at a height of 5 m above the ground next to the trailer. The sample line from the tower to the instrument was approximately 2 m. Ambient air was sampled via a $PM_{2.5}$ cyclone (*URG* 2000-30EN) at 10 l/min and through 14.1 mm ID copper tubing. The tube diameter was chosen to minimize losses by impaction and gravitational settling, for the given flow rate. Transport losses depending on particle size were calculated using simple formulas for diffusion, gravitational settling, and impaction losses (Hinds 1999) for the inlet geometry. For 20 nm particles the losses are about 3%, dominated by diffusion; at 2.5 μm the impaction and settling dominated losses are just above 5%. The minimum of losses are less than 0.3% for 260 nm particles, resulting in an unweighted average transport loss in the sampling tube of particles in the size range transmitted into the AMS of 1.3%.

At the entrance of the AMS inlet, a sample flow of 0.4 l/min is isokinetically extracted from the 10 l/min transport flow. 0.3 l/min of the sample flow is diverted to a Condensation Particle Counter (CPC) (*TSI* 3025), while 0.1 l/min is introduced into the AMS inlet. Due to the very low flow rate, the transport losses within the first few centimeters of the AMS inlet entrance are larger for small particles than in the copper tube: 6.5% for 20 nm particles and about 3.3% for 2.5 μm particles, with a minimum of 0.4% around 450 nm. The average loss in this part of the inlet is about 1.9%. Including the relatively small losses of the isokinetic sampling probe, the calculated range of the total inlet losses are about 11% for 20 nm and 9% for 2.5 μm particles, with a minimum of 0.7% for 350 nm particles. The average total transport losses for the particle diameter range from 20 nm to 2.5 μm are 3.5%. In Figure 1 the particle size dependence of the transport losses are plotted for the size range 0.02 μm to 2.5 μm for the copper inlet line, the AMS inlet, and the total inlet system (which includes the isokinetic sampling probe—not drawn separately in the graph).

For quality assurance a set of calibrations was performed before the campaign in the laboratory, as well as in the field on a regular basis. A detailed description of these calibration procedures is given in Drewnick et al. (2003).

In the field the AMS was operated to regularly switch with a 20 s cycle between the ToF mode (size information for preselected masses) and the MS mode (complete mass spectrum for bulk aerosol). Every 10 min the mass spectrum and size distribution averages were saved to disk.

In the ToF mode the particle beam was chopped with the chopper at a frequency of 120 Hz. The chopper wheel consists of an aluminum disc with two slits, allowing for a 2% duty cycle, resulting in a starting time uncertainty of the particles of 0.17 ms. Typical particle flight times for travel through the sizing chamber onto the heater are 2 to 4 ms, resulting in a potential relative error in the velocity measurement of 4–8%, which transforms into a particle diameter error of approximately the same range.

For size distribution measurements, the quadrupole mass spectrometer was set to the specific masses associated with an aerosol chemical species of interest and the ion signal at each mass was measured with 50 μs time resolution. The time-of-flight signal was measured continuously over 40 chopper cycles for every selected mass of interest.

From the first day of the campaign until 5 July at 16:30 the masses m/z = 30, 32, 46, 48, 55, 57, and 64 amu were used for size-distribution measurements. Starting on 5 July at 16:40, the masses at m/z = 15, 69, 71, 80, and 123 amu were also measured. The m/z = 32 amu (O_2^+) was used for monitoring of the multiplier gain; m/z = 15 amu (NH^+) is associated with ammonium; m/z = 30 and 46 amu (NO^+, NO_2^+) were used to determine the nitrate size distribution. The masses at m/z = 48, 64, and 80 amu (SO^+, and SO_2^+, and SO_3^+) are related to sulfate, and m/z = 55, 57, 69, 71, and 123 amu (several molecular fractions) are related to organic aerosol particles. For measurement of the organics size distribution, masses that had the largest signal-to-noise ratio in the mass spectrum were selected.

Transformation of the measured particle velocities v_p into aerodynamic particle diameters D_{aero} was done, using the following expression given in Jayne et al. (2000):

$$v_p = \frac{v_g}{1 + (D_{\text{aero}}/D^*)^b}, \qquad [1]$$

where v_g is the gas velocity at the exit of the aerodynamic lens. D^*, b, and v_g are fit parameters that were determined in the ToF calibration performed in the ASRC aerosol generation and calibration facility (Hogrefe et al. 2003) before the campaign. For this ToF calibration, size-distribution measurements of monodisperse ammonium nitrate aerosol generated by atomization of NH_4NO_3 solution and size selected with a Differential Mobility Analyzer (DMA) were performed for a variety of nominal particle sizes. Mobility diameters as determined by the DMA were converted into aerodynamic diameters using the particle density (1.72 g/cm^3) and a shape factor of 1.18. This shape factor was determined in laboratory experiments by comparison of aerodynamic properties of ammonium nitrate particles with polystyrene latex (PSL) particles of known size. In addition, size-distribution measurements of calibrated PSL particles (Duke Scientific Corp., Palo Alto, CA) of 100, 200, and 350 nm diameter were used for quality assurance. The relative uncertainty of this size measurement is dominated by the uncertainty of the particle start time due to the width of the chopper slit and by changes in particle velocity due to changes in ambient pressure. The uncertainty of the particle start time results in an uncertainty of particle diameter on the order of 8%. The particle diameter uncertainty due to weather-induced ambient pressure changes can be up to 7% (Bahreini et al. 2003). This results in an overall uncertainty of the particle diameter of about 11%.

With this approach to size-distribution measurement using the ion signal and the flight times of the particles, a direct mass-weighted size-distribution measurement of the aerodynamic particle diameters is obtained. The size distribution measurements are limited for small and large particles due to the reduced transmission of the aerodynamic lens below 60 nm and above 600 nm. While typically only a very small fraction of the aerosol mass is found for particles with diameters below 60 nm, a significant amount of particulate mass is lost due to the limited transmission of the AMS inlet lens between 600 nm and 2.5 μm. In Figure 2 the inlet transmission function as determined by FLUENT calculations is plotted in the background of the average size distributions measured over the whole campaign. Since reliable measurements of the inlet transmission function are not available at this time, no corrections to the measured size distributions for losses in the aerodynamic lens were attempted. Given the inherent limitation of the aerodynamic lens and our inability to correct for this limitation, one should keep in mind that it is difficult for the AMS to obtain an accurate measurement of the size distributions for large particles (>600 nm).

Reported size distributions are based on the conversion of the ToF distributions into aerodynamic particle size distributions

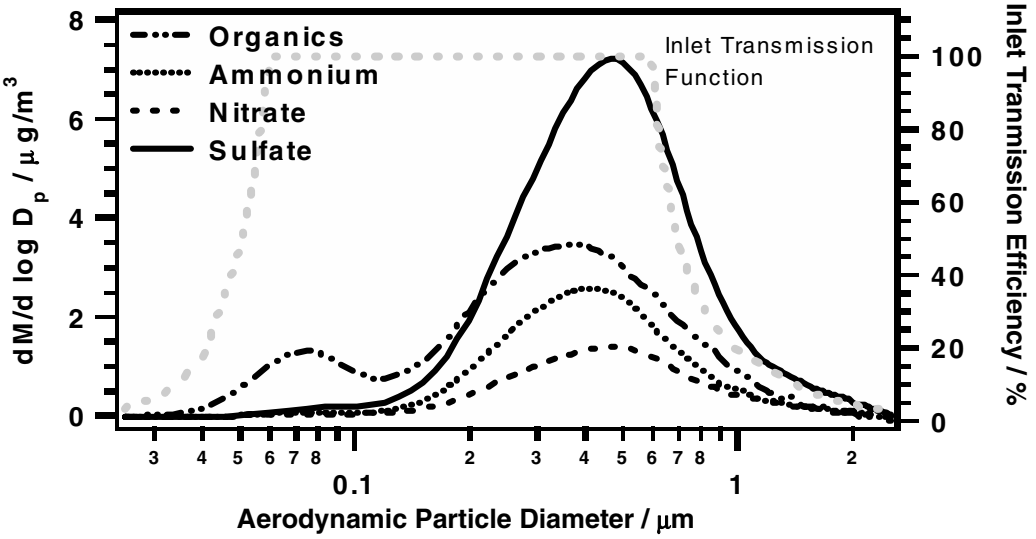

Figure 2. Average size distributions for nitrate, sulfate, ammonium, and "organics," for the whole campaign. The gray dotted line is the inlet transmission function calculated for the aerodynamic lens used to focus the particles into a narrow beam.

using the ToF calibration. This dM/dDp distribution is converted into a $dM/d \log_{10} D_p$ distribution using (Seinfeld and Pandis 1998)

$$\frac{dM}{d \log_{10} D_p} = 2.303 \cdot D_p \cdot \frac{dM}{dD_p}. \quad [2]$$

According to this transformation formula the noise of the size-distribution measurement increases with increasing particle diameter, resulting in the relatively high noise level at the large particle end for some of the size distributions shown here.

While most species are represented by a large number of fragments in the mass spectra, the size distribution measurements were only performed at a few representative masses for every species. Therefore for calculation of the absolute intensity of the size distributions shown in this article the mass concentrations measured in the mass spectrum mode during the same time interval were used. The size distributions were averaged for the time periods reported on the graphs using time as the x axis. For reduction of noise, all size distributions were smoothed using a binomial smoothing algorithm (Marchand and Marmet 1983) implemented into the IGOR PRO package (Wavemetrics), which was used for data processing. Mass-concentration calculation procedures and detection limits of the various species are described in Part I (Drewnick et al. 2003). Relative uncertainties of the mass concentration measurements were estimated to be on the order of 10–20%.

RESULTS AND DISCUSSION

The AMS was operated during this campaign from 30 June 15:00 until 6 August 18:00. During this time period valid data was collected for more than 93% of the total time, producing an almost continuous stream of 10 min averages of mass concentrations and size distributions. The missing 7% of data are mainly due to failure of the data acquisition computer (75%) and, to a minor extent, to calibration and maintenance procedures (25%). No measurement time was lost due to failure of the instrument itself.

A summary of the size distribution data is presented in Figure 2, showing the average size distribution of the nitrate, sulfate, ammonium, and "organic" particle fraction. The ammonium size distribution was compiled from the ToF data measured at m/z = 15 amu. Since this mass was measured in the ToF mode starting several days after the beginning of the campaign, the ammonium size distribution shown in this graph is just the average for the period from 5 July until the end of the campaign. For calculation of the nitrate and sulfate size distributions, ToF measurements of m/z = 30 and 46 amu and of m/z = 48, 64, and 80 amu were used, respectively. The "organic" size distribution was calculated from ToF data of m/z = 55, 57, 69, and 71 amu. While the size distributions of ammonium, nitrate, and sulfate are calculated from almost all relevant masses associated with the individual species, the "organic" size distribution is calculated from just a few of the large amount of relevant masses associated with organic particles. Since different masses are associated with different organic particle types, the size distributions measured at different "organic" masses could vary. According to this limitation, the "organic" size distribution is only one of possibly several slightly different size distributions, all associated with organic particles. Since some of the most prominent masses from the organic mass spectrum are used to calculate this "organic" size distribution, it will not differ significantly from the "true" organic size distribution most of the time, and the long-term average should be very close to the true distribution. To account for different size distributions measured at different masses, the total organics size distribution for any given time period was calculated by adding the four size distributions of the selected masses, weighted according to their average relative mass concentrations during this time period.

While the typical size distribution of ammonium, nitrate, and sulfate particles consists primarily of a single mode of accumulation-mode particles, the organics size distribution most typically has two modes, an accumulation mode and a small particle mode. For determination of mode diameters and distribution widths Gaussian fits were performed for the size distributions in Figure 2 over a logarithmic particle diameter axis. These fits indicate that the measured size distributions are well described by the log-normal function.

According to these fits the mode of the average nitrate size distribution is at 439 nm, and its width (standard deviation of fitted gauss function) is 615 nm. Sulfate peaks at 447 nm with a width of 625 nm. Within the relative uncertainty of the size measurement (11%), these mode diameters agree well with each other. The maximum of the ammonium size distribution is found at a slightly smaller diameter, at 400 nm. Its width of 564 nm is somewhat narrower than that of sulfate and nitrate. The organic particle size distribution has two modes with diameters of 78 nm and 359 nm and widths of 78 and 710 nm, respectively.

The very similar results for average-mode diameter, as well as size-distribution width of the nitrate and the sulfate size distributions, indicate that these two particle types are internally mixed. This conclusion is also supported by the hourly averages of the size distributions and their trends in time (not shown). In most of the periods the nitrate and the sulfate size distribution have similar mode diameters, similar distribution widths, and similar shapes. Moreover, if one of these two size distributions has an unusual shape, the other one typically has it, too.

The ammonium size distribution peaks at a slightly smaller particle diameter than sulfate and nitrate, indicating that this size distribution is associated not only with nitrate and sulfate but also with organic particles (that are typically even smaller than the ammonium particles). This could either be due to ammonium associated with organic particles or to an organic interference at m/z = 15 amu.

On the other hand, the "organic" size distributions are substantially different than those of the inorganic species, as shown in Figure 2. With an average mode diameter of 358 nm, the accumulation-mode peak occurs at a significantly smaller particle diameter than nitrate, sulfate, and even ammonium. In

addition, at almost all time intervals a small diameter mode around 80 nm is observed. This small particle mode and the relatively small diameter of the accumulation mode are indicative of relatively young aerosol, likely produced locally by the huge amount of traffic in the vicinity of the measurement site. Furthermore, this traffic-related organic aerosol is not (or only to a minor extent) internally mixed with the more aged ammonium sulfate and ammonium nitrate aerosol. This conclusion is supported by the fact that there is little similarity in the shape of the organic and sulfate/nitrate size distributions in the hourly averages (not shown).

Bimodal organic size distributions were already found in earlier measurements with the AMS in Manchester, UK. In these measurements the small particle mode was associated with hydrocarbon-like species, while the larger mode mainly consisted of oxidized species (Allan et al. 2003).

In addition to the average size distributions of the individual species, the inlet transmission function of the aerodynamic lens is shown in Figure 2. This function was calculated with FLUENT for the aerodynamic lens assembly used in this campaign. The calculated cutoff for small particles below approximately 60 nm appears to be confirmed by the organic small-particle mode that was never found at particle diameters significantly below the ones shown in the average size distribution. Even at very high mass loadings in this small particle mode (Figure 3a) no extension to smaller particles is observed, indicating that this lower end of the size distribution is likely due to a particle transmission cutoff rather than a real feature of the size distribution of the organic particles. A new lens design under development at Aerodyne Research, Inc. is expected to resolve the small-particle transmission issue.

The excellent fit of the log-normal function to the sulfate size distribution in Figure 2 suggests that the inlet transmission cutoff for large particles above 600 nm is less sharp than the calculated cutoff and is indicative of significantly higher particle transmission for large particles than the calculation would indicate.

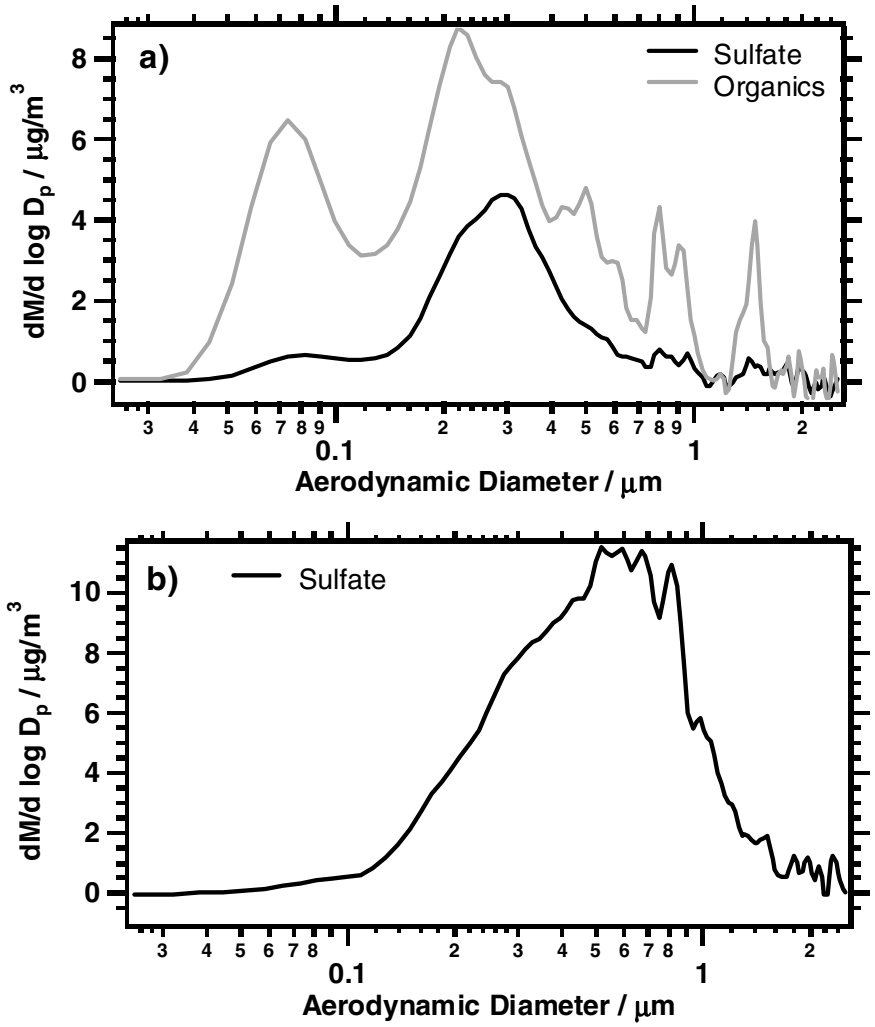

Figure 3. Sulfate and organics size distributions with mass predominantly at (a) relatively small particle sizes (measured on 7/7/01 6:00–8:00); and a sulfate size distribution with mass predominantly at (b) relatively large particle sizes (measured on 7/25/01 8:00–10:00).

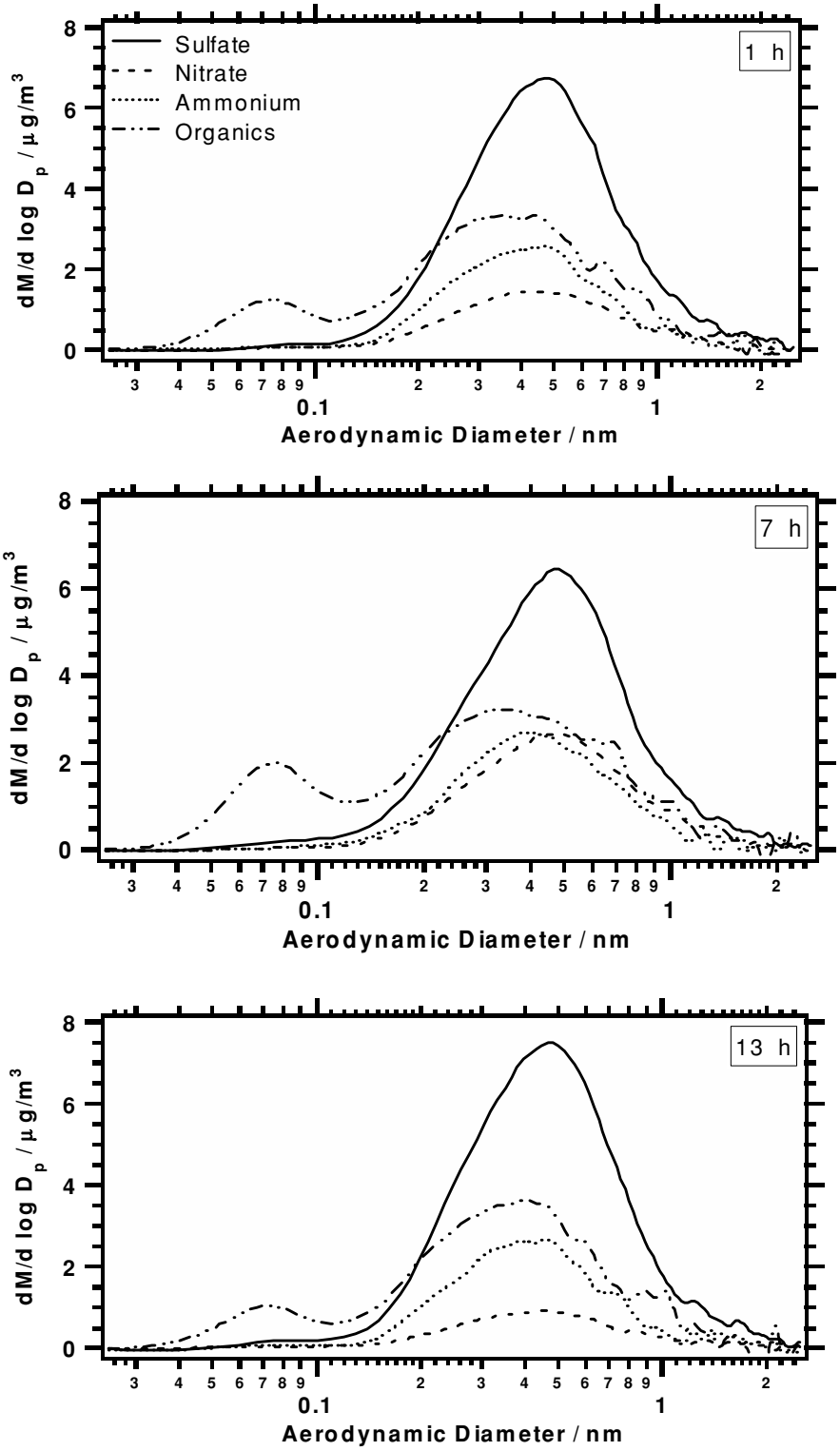

Figure 4. Diurnal patterns of the size distributions of sulfate, nitrate, and organics. Four examples, separated by 6 h are shown: 1:00–2:00 h, 7:00–8:00 h, 13:00–14:00 h, and 19:00–20:00 h. *(Continued)*

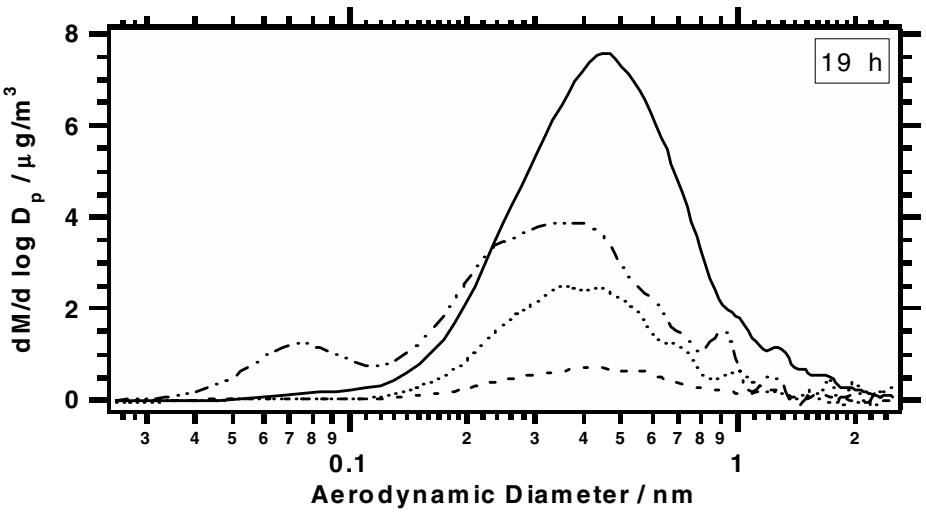

Figure 4. (Continued)

Sulfate size distributions are shown in Figure 3 for a small-mode diameter (Figure 3a) and a relatively large mode diameter (Figure 3b). While the size distribution in Figure 3a seems not to be affected by the large-particle cutoff of the AMS inlet system, some effects of this cutoff can be seen in the size distribution in Figure 3b. From this distribution it can be estimated that the cutoff of the inlet system starts at particle diameters somewhere in the range of 800–1000 nm.

The diurnal patterns of the size distributions of nitrate, sulfate, and organics were calculated by averaging all size distributions measured over each specific hour of the day for the entire campaign. Examples of the size distributions for four 1 h periods (starting at 1:00, 7:00, 13:00, and 19:00) distributed over the day are shown in Figure 4.

Considering the size distribution data of all hours of the day, no significant change in the mode diameter of the nitrate or sulfate size distribution was found. Also, the maxima of the two modes of the organics size distribution do not change during the course of the day.

The absolute intensity of the size distributions show the variations already found in the diurnal patterns of the mass concentrations (Drewnick et al. 2003) with a clear maximum of the nitrate mass concentration during the early morning hours, small maxima of the organics mass concentration during rush-hour times, and almost no changes of the sulfate concentration.

As mentioned previously, the organic size distributions consist of two clear modes: an accumulation mode at about 350 nm and an intensive small-particle mode around 80 nm. A clear pattern was found for the small-particle fraction of organic particles, as depicted in Figure 5.

Figure 4 also shows that during the early morning hours the small-particle mode of the organic particles is particularly

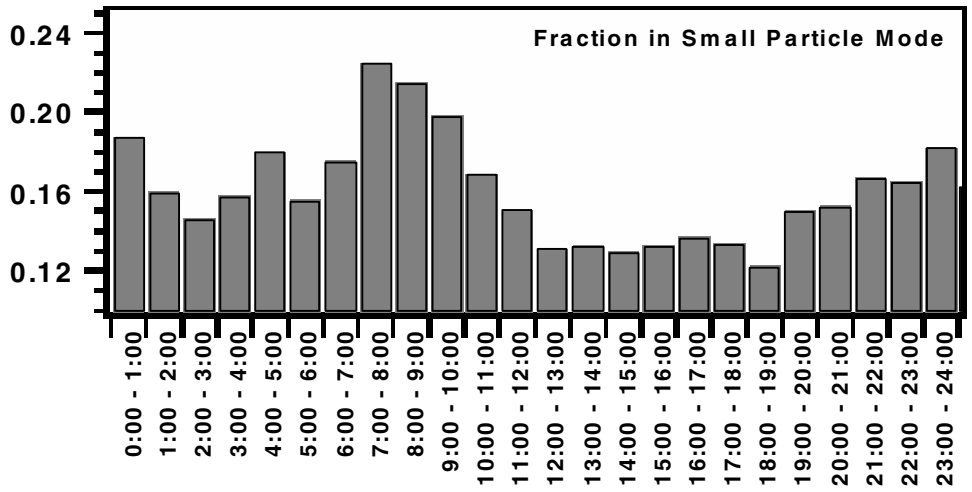

Figure 5. Diurnal pattern of the fraction of the organic particle mass found in the organics small-particle mode with particles below 120 nm.

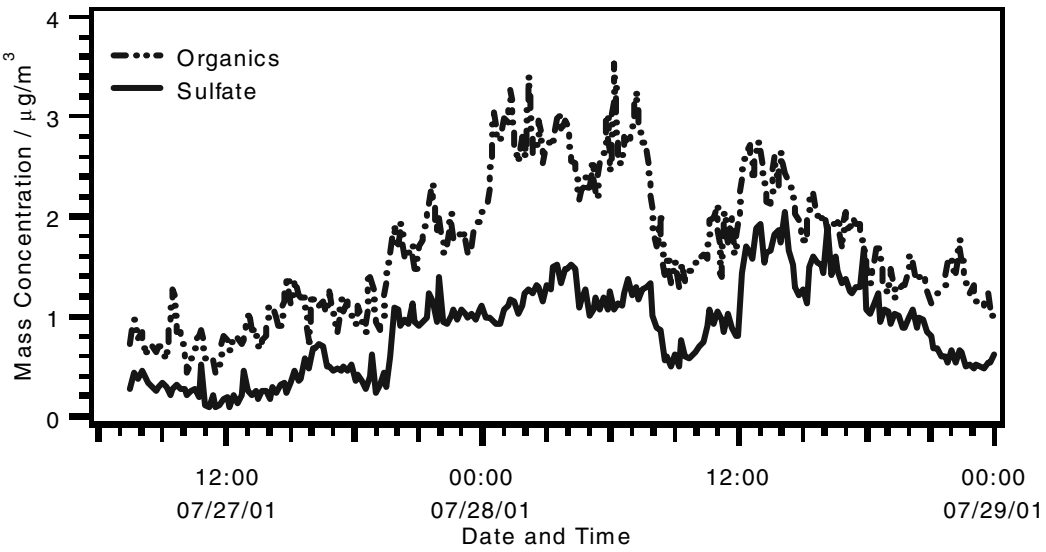

Figure 6. Mass concentration time series for sulfate and organics for the interval covered by the size distribution data in Figure 7.

intense, with a large fraction of the organic mass concentration found in this mode (up to 22% of the total organic mass). The relative intensity of the small-particle mode decreases until noon and then slowly increases again during the afternoon, with a faster increase during the evening. From AMS mass concentration measurements performed during this campaign (see part I) two types of organic particles with distinct diurnal cycles were identified. One type is associated with photochemical production of secondary organic particles, while the other is associated with traffic-related primary organic particles. The traffic-related organic fraction has the same diurnal trend as that found for the organic small-particle mode, suggesting that this mode is dominated by vehicle particulate emissions from nearby highways during the morning and evening rush hours.

While the sulfate and nitrate size distributions are predominantly monomodal with an accumulation mode at about 450 nm, both size distributions also show a very weak small-particle mode with particles below 100 nm.

Gas-to-particle conversion is the principal source of sulfate in particles (Seinfeld and Pandis 1998). In the first step SO_2 vapor is oxidized by OH to sulfur trioxide (SO_3), followed immediately by reaction with water to form sulfuric acid. Sulfuric acid vapor can undergo homogeneous nucleation, resulting in new particle formation, or condense on pre-existing particles. The competition between these two processes is dependent on the ambient aerosol size distribution and the sulfuric acid formation rate. In the presence of ammonia and water vapor, sulfuric acid is converted into ammonium sulfate. These processes lead to particle growth by further condensation and by coagulation of small particles. These growth mechanisms eventually become inefficient, leading to the accumulation mode with diameters on the order of a few hundred nm.

Sulfate deposition onto (or formation of) small particles contributes significantly to aerosol loading only during periods of very low ambient particulate sulfate concentrations. Figure 6, displays a time series of sulfate and organics mass concentrations measured with the AMS, which shows such an event (Drewnick et al. 2003). During the time period shown in Figure 6, the organics mass concentration is significantly higher than the sulfate concentration. The typical size distribution of organic particles measured during this campaign suggests the presence of a significant small particle mode over the whole time interval.

The capability of the AMS to measure size distributions of different species independently enables the resolution of the small particle mode of the sulfate particles associated with the sulfate event presented in Figure 6 despite the large background of small organic particles. This is a significant advantage over any particle size measurement techniques that are unable to provide simultaneous chemical speciation (e.g., SMPS measurements) and thus are not able to differentiate between the small sulfate particle mode and the small organic particle mode.

A series of 2 h averages of the sulfate size distributions for this time period are shown in Figure 7. The first column of size distributions are shown with an extended y axis scaling due to the low sulfate mass concentration during the first hours of this event. The very low total concentration and the conversion from the ToF data into $dM/d\log_{10} D_p$ data (Equation (2)), results in a significant increase in the noise level at large particle sizes that cannot be interpreted as real features of the sulfate size distribution. At the start of Figure 7 (7/27 8:00–12:00), before sulfate loading has begun to increase, the sulfate size distribution consists mainly of an accumulation mode that is smaller in both loading and size than that typical during high sulfate loadings (i.e., 300 versus 450 nm diameter). The sulfate mass concentration slowly starts to increase after 12:00 with the increasing mass appearing in a new small-particle mode, ~70–80 nm diameter. The intensity of this small-particle mode increases,

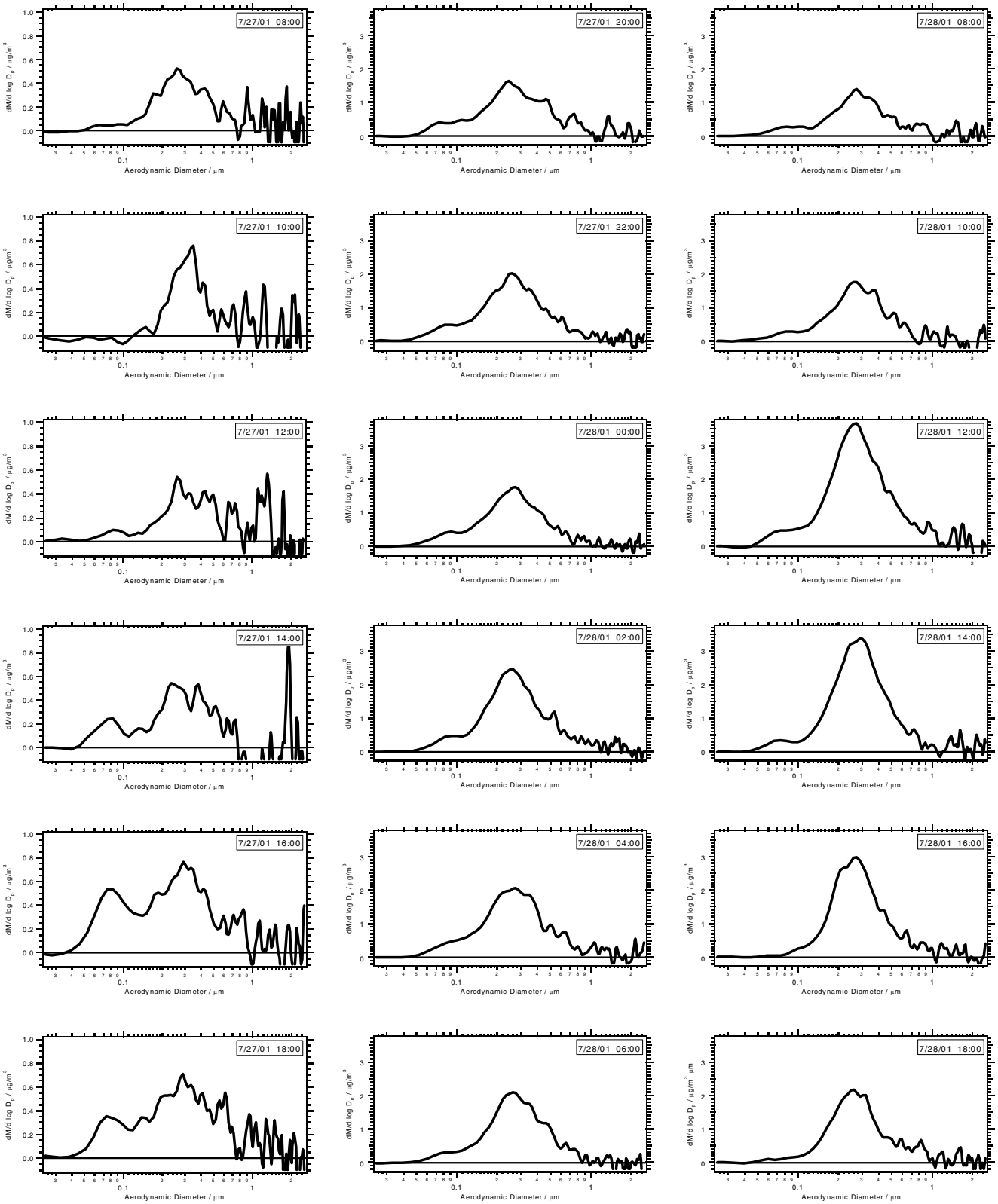

Figure 7. Two-hour averages of the sulfate particle size distribution during the period displayed in Figure 6, from 7/27/01 8:00 until 7/28/01 20:00 (displayed times are the start times of the intervals). Data are printed in columns. Note: the scale of the *y* axis changes after the first column due to the increased mass concentrations during the following intervals.

and increasing sulfate also appears in the accumulation mode (between 100–200 nm) as these small particles grow to larger sizes.

Later that night, when the sulfate mass concentration reached a plateau (starting at 20:00), the small particle mode appears to merge with the accumulation mode (7/28 4:00).

After some decreases of the mass concentration later in the morning of 7/28, the mass concentration again rises, accompanied by a similar intensification of the sulfate small-particle mode. After 14:00 on this day, the sulfate event subsides and the remaining small-particles continue growing, causing the small-particle mode eventually to disappear into the accumulation mode while the size distribution narrows, matching the distribution at the start of Figure 7.

This series of size distributions clearly shows some further advantages of the AMS over traditional techniques. Similar information could be obtained with MOUDI samples. However, the time resolution would be in the order of 12 h, resulting in an averaging out of most of the size-distribution evolution. In addition, with MOUDI samples the size distribution would be binned in a series of relatively large size bins, hiding most of the details of the size-distribution evolution.

Figure 8 shows a time series of size-distribution mode diameter of aerosols containing sulfate, nitrate, and organics. The high correlation between the positions of the size-distribution maxima of nitrate and sulfate aerosols suggests that sulfate and nitrate are internally mixed. In contrast, the mode diameters of the organic particles show less correlation with nitrate and sulfate, supporting the assumption that partial external mixture of these species exist.

It is important to note that the organics small-particle mode (not shown in Figure 8) is constant over the period of the whole campaign. This probably does not reflect the exact evolution of the small-particle mode but supports the assertion that the position of the measured small-particle mode reported here is largely determined (or at least influenced) by the inlet transmission cutoff of the aerodynamic lens at small particle sizes.

Comparison of the time series of modes of the size distributions of the individual species and their mass concentrations (Figure 8) shows a significant relationship between these quantities: In general the mode diameter of the accumulation mode particles increases when the mass concentration of the species increases. After the end of a high mass concentration event, the mode diameter decreases again. These differences in mode diameter likely reflect the age of the aerosol. Based on results from the mass concentration measurements (Drewnick et al. 2003), the pollution events are primarily related to regional transport rather than to intense local production. This suggests that the aerosol observed during these events is dominated by aged aerosol that has been transported to the site and is consistent with the observed larger mode diameter size distributions. During times of low total mass concentrations, the locally produced fraction of young and small particles play a larger role in the aerosol size distribution, shifting the mode diameter to smaller sizes.

For the sulfate and organic size distributions this correlation between mode diameters and mass concentration is observed

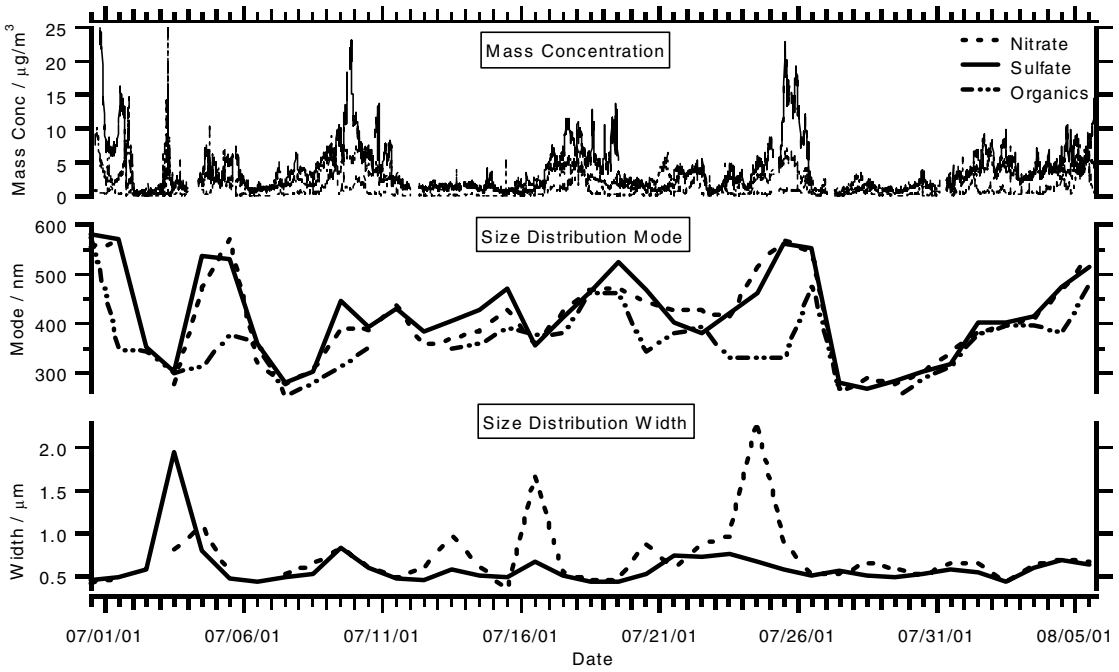

Figure 8. Time series of nitrate, sulfate, and organics mass concentration for the whole campaign, together with time series of the mode diameters of these species and size distributions widths for nitrate and sulfate size distributions. The mass concentration data have 10 min resolution; the size distribution data are averaged for 24 h periods.

very clearly. However, the nitrate mode diameters in Figure 8 do not follow these trends exactly. A much better relationship is observed between the nitrate mode diameters and the sulfate mass concentration. This observation is consistent with an internal mixture of nitrate- and sulfate-containing particles such that the mode diameter of the nitrate-containing particles is mainly determined by the dominant sulfate size distributions and therefore related to the sulfate mass concentration trends. Since ammonium sulfate has a low vapor pressure, it is fairly independent of thermodynamic conditions. In contrast, ammonium nitrate mass concentrations are highly dependant on thermodynamic conditions. Typically, once aerosol sulfate is fully neutralized, any remaining gas-phase ammonia forms ammonium nitrate, which then condenses onto the pre-existing sulfate aerosol. This process results in a coincidence of sulfate and nitrate mode diameters and a dependence of both mode diameters on the sulfate mass concentration.

While some correlation between the widths of the sulfate and the nitrate size distributions (Figure 8, bottom part) is also observed, there are some events when the nitrate size distribution is significantly broader than the sulfate size distribution. These events occur during times of extremely low nitrate concentration

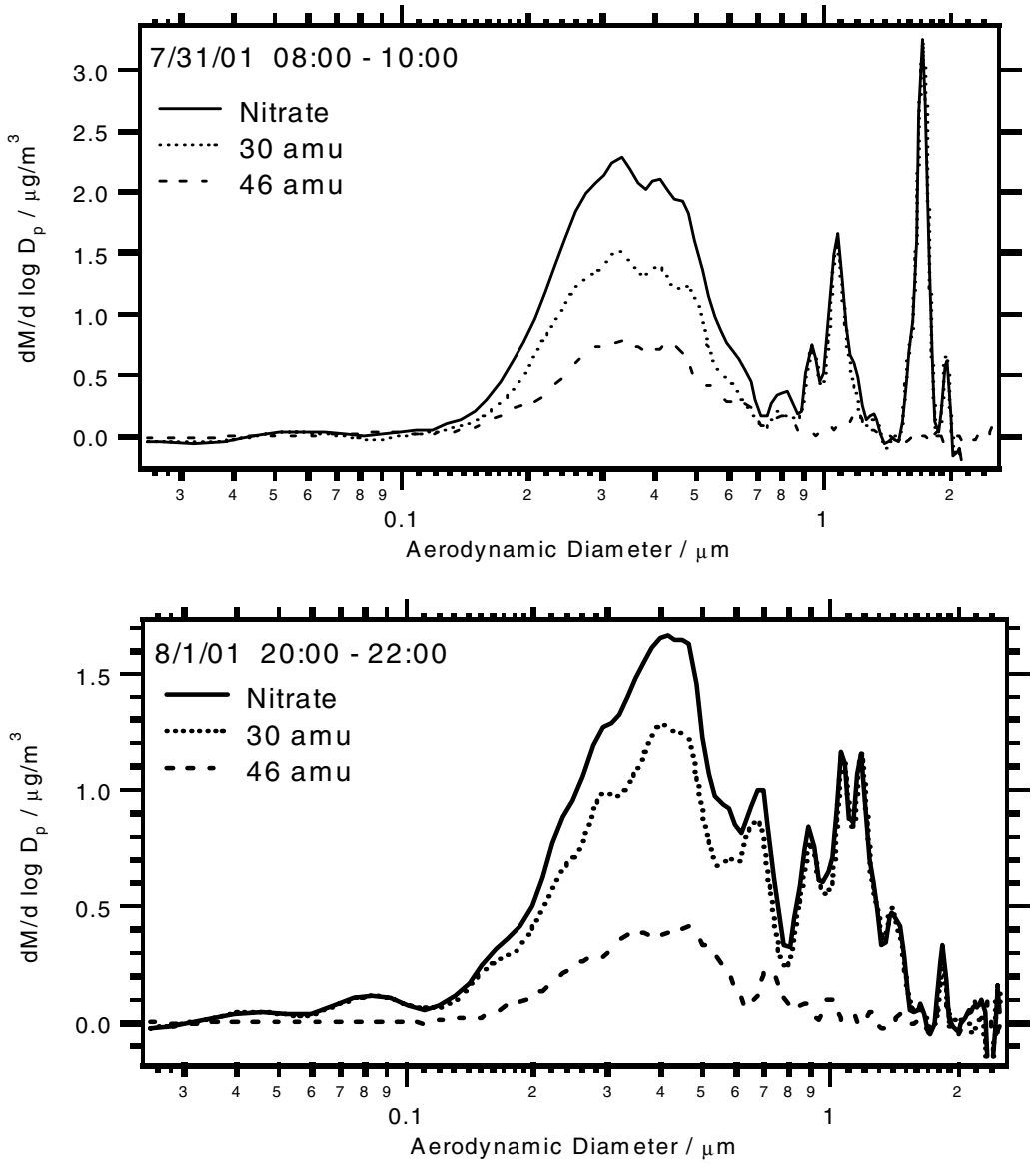

Figure 9. Two-hour averages of the nitrate size distribution measured on 7/31/01 from 8:00–10:00 and on 8/01/01 from 20:00–22:00. In addition to the nitrate size distribution, the size distributions of the nitrate fractions at m/z = 30 and 46 amu are printed. Note that for the largest particles, nearly all the nitrate comes from m/z = 30, in clear contrast to the particles in the size range below 600 nm.

when there is a relatively weak small-particle mode, which grows into the accumulation mode and results in a broadening of the total size distribution.

The nitrate mass spectrum signal is the sum of the signals at m/z = 30 amu (NO^+) and 46 amu (NO_2^+). Accordingly, the nitrate size distribution is the sum of the size distributions measured at m/z = 30 and 46 amu. Most of the nitrate measured in the accumulation mode is present in the form of ammonium nitrate, formed by gas-to-particle conversion processes and subsequent growth of the particles by condensation and agglomeration. For ammonium nitrate particles, the ratio of the signal at the two main fractions at m/z = 30 amu and at m/z = 46 amu is approximately 2:1. This signal ratio is also found for most of the size distribution data in the accumulation mode. However, during some time periods large nitrate particles were detected with signal predominantly at m/z = 30 amu (NO^+), as shown in the two examples in Figure 9.

In Figure 9 the nitrate size distributions averaged for the time periods of 7/31/01 8:00–10:00 and 8/01/01 20:00–22:00 are plotted together with the two fractions representing the nitrate size distribution measured at m/z = 30 and 46 amu, respectively. The solid top curve in both graphs is the combined nitrate size distribution, calculated by addition of m/z = 30 amu (dotted) and m/z = 46 amu (dashed) size distributions.

In the accumulation mode, between ~100 nm and 700 nm for both nitrate size distributions, the typical nitrate fractionation pattern of ammonium nitrate with a ratio of 2:1 in the intensities of m/z = 30 amu to m/z = 46 amu signal is found, indicating that these nitrate particles contain ammonium nitrate. However, a different m/z = 30- to -m/z = 46 ratio is found for the larger nitrate particle modes that occur from 700–2000 nm. This different fragmentation pattern of the large nitrate particles can be explained using laboratory AMS measurements, performed in our lab (unpublished) and elsewhere (UMIST 2001, personal communication), of nitrate fragmentation patterns for different nitrate salts. A nitrate fractionation pattern with almost no signal at m/z = 46 amu is typically found for low vapor pressure nitrate salts like $NaNO_3$, KNO_3, or $Ca(NO_3)_2$. Thus, the most likely explanation for these large nitrate particles is that they are $Ca(NO_3)_2$ particles, which are products from crustal materials ($CaCO_3$ converted to $Ca(NO_3)_2$ by nitric acid) generated by mechanical processes. This explanation is supported by the fact that in speciation data from filters collected during the campaign calcium concentrations are high typically during days on which these large nitrate particles were found.

Due to the different generation process of the $CaNO_3$ particles compared to the ammonium nitrate generation process, these particles have much larger diameters than most of the ammonium nitrate particles measured during this campaign. The sensitivity of the AMS to these particles is greatly reduced by the low inlet transmission efficiency of the aerodynamic lens system for large particle sizes. Since the AMS lens transmission for large particles has not been quantitatively determined by experimental measurements, estimates of the influence of these particles on the nitrate mass concentration cannot be made at this time.

SUMMARY AND OUTLOOK

The AMS was successfully deployed during the PMTACS–NY 2001 summer campaign in Queens/New York in summer 2001, obtaining 10 min averages of aerosol bulk mass spectra, and sulfate, nitrate, ammonium, and organics size distributions.

Based on average mass weighted size distributions for the whole campaign (as well as short time averages), it is hypothesized that nitrate and sulfate particles appear mainly as ammonium nitrate and ammonium sulfate and are internally mixed. Both species typically appear in a single mode with maximum around 440 nm. The monomodal ammonium size distribution is shifted towards a mode diameter of 400 nm. This is either due to ammonium associated with organic particles or to organic interferences at m/z = 15 amu. A completely different size distribution is found for the organic particles with two modes at 80 and 360 nm, respectively.

Diurnal patterns of the size distributions of sulfate, nitrate, and organic particles show little change of mode diameter during the day, suggesting that most of this aerosol mass is transported to the measurement site from a different region. The intensities of the size distributions vary over the course of the day according to the diurnal patterns of the mass concentrations (Drewnick et al. 2003). The most significant pattern was found for the fraction of organic particles in the small particle mode (particle diameters below 120 nm). This fraction showed a large maximum during the morning rush hour, when the most traffic was experienced in the highways around the site and especially in the parking lot next to the site. Smaller maxima were found for the afternoon rush hour and the evening traffic. These results suggest that the appearance of the intense small-particle mode in the size distribution of the organic particles is caused by the heavy traffic on the highways and the parking lot around the measurement site. A complete analysis of the diurnal variation in aerosol loading needs to take into account local meteorology, including day/night changes in boundary layer height and mixing.

Comparison of time series of the mode diameter of sulfate, nitrate, and organics with mass concentration data gives additional insight into the evolution processes of the aerosol and indicates that nitrate and sulfate are internally mixed in the aerosol particles. The mode diameters of the organic particles show less correlation with those of nitrate and sulfate, supporting the assumption of at least partial external mixture of these species.

In addition, these time series give insight into the evolution processes of the aerosol. The ability to measure the size distributions of individual species separately provides the opportunity to track the varying degrees of evolution of chemically distinct particles that have similar sizes (i.e., small sulfate particles from photochemical production versus small organic particles from local emissions). This is a unique attribute of the AMS since this type of analysis is not possible with standard aerosol particle counting and sizing instrumentation.

Additional studies in progress using the AMS data from this campaign includes further investigation of these particle production events and comparison of measured production rates of particulate sulfate with calculated production rates derived from gas measurements.

REFERENCES

Allan, J. D., Coe, H., Bower, K. N., Williams, P. I., Gallagher, M. W., Alfarra, M. R., Jimenez, J. L., Nemitz, E., McDonald, A. G., Canagaratna, M. R., Jayne, J. T., and Worsnop, D. R. (2003). Quantitative Sampling Using an Aerodyne Aerosol Mass Spectrometer 2: Measurements of Fine Particulate Chemical Composition in Two UK Cities, *J. Geophys. Res.* 108(D3):4091.

Allen, G. A., Harrison, D., and Koutrakis, P. (2001). A New Method for Continuous Measurement of Sulfate in the Ambient Atmosphere, *American Association for Aerosol Research, 20th Annual Conference*, October 2001.

Allen, J. O., Fergenson, D. P., Gard, E. E., Hughes, L. S., Morrical, B. D., Kleeman, M. J., Gross, D. S., Galli, M. E., Prather, K. A., and Cass, G. R. (2000). Particle Detection Efficiencies of Aerosol Time of Flight Mass Spectrometers Under Ambient Sampling Conditions, *Environ. Sci. Technol.* 34(1):211.

Bahreini, R., Jimenez, J. L., Jayne, J. T., Worsnop, D. R., Flagan, R. C., and Seinfeld, J. H. (2003). Aircraft-Based Aerosol Mass Spectrometer Measurements of Particle Size and Composition During ACE-Asia, *J. Geophys. Res.—Atmos.* 108:8645.

Carson, P. G., Johnson, M. V., and Wexler, A. S. (1997a). Real-Time Monitoring of the Surface and Total Composition of Aerosol Particles, *Aerosol Sci. Technol.* 26:291–333.

Carson, P. G., Johnston, M. V., and Wexler, A. S. (1997b). Laser Desorption/Ionization of Ultrafine Aerosol Particles, *Rapid Comm. Mass Spec.* 11:993–996.

Drewnick, F., Schwab, J. J., Jayne, J. T., Canagaratna, M., Worsnop, D. R., and Demerjian, K. L. (2004). Measurement of Ambient Aerosol Composition During the PMTACS–NY 2001 Using an Aerosol Mass Spectrometer, Part I: Mass Concentrations, *Aerosol Sci. Technol.* 38:92–103.

Finlayson-Pitts, B. J., and Pitts Jr., J. N. (1997). Tropospheric Air Pollution: Ozone, Airborne Toxics, Polycyclic Aromatic Hydrocarbons and Particles, *Science* 276:1045–1051.

Gard, E., Mayer, J. E., Morrical, R. D., Dienes, T., Fergenson, D. P., and Prather, K. A. (1997). Real-Time Analysis of Individual Atmospheric Aerosol Particles: Design and Performance of a Portable ATOFMS, *Anal. Chem.* 69:4083–4091.

Gross, D. S., Galli, M. E., Silva, P. J., and Prather, K. A. (2000). Relative Sensitivity Factors for Alkali Metal and Ammonium Cations in Single Particle Aerosol Time-of-Flight Mass Spectra, *Anal. Chem.* 72:416–422.

Hinds, W. C. (1999). *Aerosol Technology: Properties, Behavior, and Measurement of Airborne Particles*, 2nd ed. John Wiley and Sons, Inc., New York.

Hizenberger, R., Berner, A., Giebl, H., Kromp, R., Larson, S. M., Rouc, A., Kock, A., Marischka, S., and Puxbaum, H. (1999). Contribution of Carbonaceous Material to Cloud Condensation Nuclei Concentrations in European Background (Mt. Sonnblick) and Urban (Vienna) Aerosols, *Atmos. Environ.* 33:2647–2659.

Hogrefe, O., Drewnick, F., Lala, G. G., Schwab, J. J., and Demerjian, K. L. (2004). Development, Operation, and Applications of an Aerosol Generation, Calibration and Research Facility, *Aerosol Sci. Technol.* 38:196–214.

Jacob, D. J. (2000). Heterogeneous Chemistry and Tropospheric Ozone, *Atmos. Environ.* 34:2131–2159.

Jayne, J. T., Leard, D. C., Zhang, X., Davidovits, P., Smith, K. A., Kolb, C. E., and Worsnop, D. R. (2000). Development of an Aerosol Mass Spectrometer for Size and Composition Analysis of Submicron Particles, *Aerosol Sci. Technol.* 33:49–70.

Jimenez, J. L., et al., Ambient Aerosols Sampling Using the Aerodyne Aerosol Mass Spectrometer, *J. Geophys. Res.* 108:8425, DOI: 10.1029/2001JD001213.

Kane, D. B., and Johnston, M. V. (2000). Size and Composition Biases on the Detection of Individual Ultrafine Particles by Aerosol Mass Spectrometry, *Environ. Sci. Technol.* 34:4887–4893.

Liu, P., Ziemann, P. J., Kittelson, D. B., and McMurry, P. H. (1995a). Generating Particle Beams of Controlled Dimensions and Divergence: I. Theory of Particle Motion in Aerodynamic Lenses and Nozzle Expansions, *Aerosol Sci. Technol.* 22:293–313.

Liu, P., Ziemann, P. J., Kittelson, D. B., and McMurry, P. H. (1995b). Generating Particle Beams of Controlled Dimensions and Divergence: II. Experimental Evaluation of Particle Motion in Aerodynamic Lenses and Nozzle Expansions, *Aerosol Sci. Technol.* 22:314–324.

Marchand, P., and Marmet, L. (1983). Binomial Smoothing Filter: A Way to Avoid Some Pitfalls of Least-Squares Polynomial Smoothing, *Rev. Sci. Inst.* 54:1034–1041.

McMurry, P. A. (2000). Review of Atmospheric Aerosol Measurements, *Atmos. Environ.* 34:1959–1999.

Murphy, D. M., and Thomson, D. S. (1997). Chemical Composition of Single Aerosol Particles at Idaho Hill: Positive Ion Measurements, *J. Geophys. Res.* 102:6341–6368.

Pope, C. A., Burnett, R. T., Thun, M. J., Calle, E. E., Krewski, D., Ito, K., and Thurston, G. D. (2002). Lung Cancer, Cardiopulmonary Mortality, and Long-Term Exposure to Fine Particulate Air Pollution, *J. Am. Med. Associ.* 287:1132–1141.

Ravishankara, A. R. (1997). Heterogeneous and Multiphase Chemistry in the Troposphere, *Science* 276:1058–1065.

Reilly, P. T. A., Lazar, A. C., Whitten, W. B., and Ramsey, J. M. (1999). Real-Time Individual Particle Analysis Using a Glow Discharge Ion Source. *18th Annual Conference of the American Association for Aerosol Research*, Tacoma, Washington.

Samet, J. M., Dominici, F., Curriero, F. C., Coursac, I., and Zeger, S. L. (2000). Fine Particulate Air Pollution and Mortality in 20 U.S. Cities, *New Engl. J. Med.* 343:1742–1749.

Seinfeld, J. H., and Pandis, S. N. (1998). *Atmospheric Chemistry and Physics: From Air Pollution to Climate Change*. John Wiley and Sons, Inc., New York.

Stolzenburg, M. R., and Hering, S. V. (2000). A New Method for the Automated Measurement of Atmospheric Fine Particle Nitrate, *Environ. Sci. Technol.* 34:907–914.

Weber, R. J., Orsini, D., Daun, Y., Lee, Y.-N., Klotz, P. J., and Brechtel, F. (2001). A Particle-into-Liquid Collector for Rapid Measurement of Aerosol Bulk Chemical Composition, *Aerosol Sci. Technol.* 35:718–727.